Electro-permeabilization of a prolate spheroidal model of biological cells

David J.N. Wall[*], **Andrew T. Shanks**[†], **and Patrick S. Bodger**[‡]

[*] *Biomathematics Research Centre, Department of Mathematics & Statistics, University of Canterbury, Private Bag 4800, Christchurch, New Zealand.*

Report Number: 185 September, 1999

Keywords: Electropororation, Laplaces equation

[†] *Department of Mechanical Engineering, University of Canterbury, Private Bag 4800 Christchurch , New Zealand.*

[‡] *Department of Electrical and Electronic Engineering, University of Canterbury, Private Bag 4800 Christchurch, New Zealand.*

Electro-permeabilization of a prolate spheroidal model of biological cells

David J.N. Wall* Andrew T. Shanks † Patrick S. Bodger‡

August 1999.

Abstract

The extent of mathematical analysis for electro-permeabilization of biological cells has thus far been constrained to spherical models. In this paper, the spherical model is extended to a prolate spheroidal balloon model, which is considered more representative of many real cells under actual field conditions.

It is shown that the size dependence of the dielectric voltage breakdown for the spheroidal cells can be eliminated. This also reduces the dependence of the breakdown on the eccentricity of the spheroidal cells over a range of shapes. It is shown that dielectric breakdown of needle shaped cells will occur at higher applied fields than spherical ones.

1 Introduction

Mathematical models of the onset of electro-permeabilization of the membrane of biological cells has been widely cited with respect to spherical models [7, 12, 14]. This is relevant to a number of simple micro-organisms or special cell types such as cysts. Furthermore, a spherical model is conceptually simple to visualize and analytically succinct.

However, many micro-organisms have elongated cell forms. Further, under application of an electric field, spherical cells may become prolate due to the compression force in a direction perpendicular to the field [1] such that the spherical model is not valid at the actual time of electro-permeabilization. Hence the simple spherical model may not be a good predictor of when electro-permeabilization will occur.

*Biomathematics Research Centre, Department of Mathematics & Statistics, University of Canterbury, Private Bag 4800 Christchurch, New Zealand. Email: D.Wall@math.canterbury.ac.nz

†Department of Mechanical Engineering, University of Canterbury, Private Bag 4800 Christchurch , New Zealand. Email: A.Shanks@mech.canterbury.ac.nz

‡Department of Electrical and Electronic Engineering, University of Canterbury, Private Bag 4800 Christchurch, New Zealand. Email: P.Bodger@elec.canterbury.ac.nz

In this paper, the spherical model is extended to a prolate spheroidal balloon model, which is considered more representative of many real cells under actual electric field conditions. Only spheroids aligned parallel to the applied electric field are considered, although both parallel and perpendicular alignments have been observed [1].

§ 2.1 describes the typical processes used in electro-permeabilization techniques and lists some basic facts. In § 3 we derive the pertinent results for the prolate spheroid model. The trans-membrane potential drop is derived from static considerations of Laplace's equation in § 3.2. This analysis is modified slightly, together with a homogenisation technique, to derive an effective time constant for the leakage of the polarisation charge from the prolate spheroid membrane in § 3.3. These two sections provide the theoretical development to enable the derivation of two important parameters used in electro-permeabilization, namely the resistivity factor and the surface charge leakage time constant. The resistivity factor, which is determined by the geometry and relative resistivities associated with the cell, is important in determining how the applied potential field is converted into a trans-membrane potential in the cell, and this in turn will model when membrane dielectric breakdown will occur. It is shown that the spheroidal eccentricity[1] does not effect this factor as much as the relative associated resistivities, and the membrane thickness. However, the spheroidal eccentricity has a major effect on the time constant associated with temporal redistribution of surface charge density, and this time constant can become very large in *needle shaped* cells.

In § 3.4 it is shown how the dependence of the dielectric breakdown on the size of the prolate spheroidal cells can be eliminated. This also reduces the dependence of the breakdown on the eccentricity of the spheroidal cells for a range of *fatter* spheroidal shapes. However, it is shown that *needle shaped* cells will have dielectric breakdown at higher applied fields than fatter ones.

Finally in Appendix A.2 we list pertinent results for the spherical balloon model, this is so that we may contrast them with the results derived in § 3.

2 Electro-permeabilization

A typical electro-permeabilization setup is shown in Figure 1, which depicts a cell suspended in a conducting medium and where electrodes are placed at each end of the medium. There are three distinctly different medium regions, outside the cell, the cell membrane, and inside the cell, denoted by subscripts o, m, i, respectively. When a large enough potential difference is applied across the outside medium, a transmembrane potential is developed. Perforation of the membrane medium may then occur.

2.1 Physical considerations

In modelling the process of electro-permeabilization, there are several physical constants which need to be measured or approximated in order to obtain *realistic* results from a

[1] Defined in § 3.1

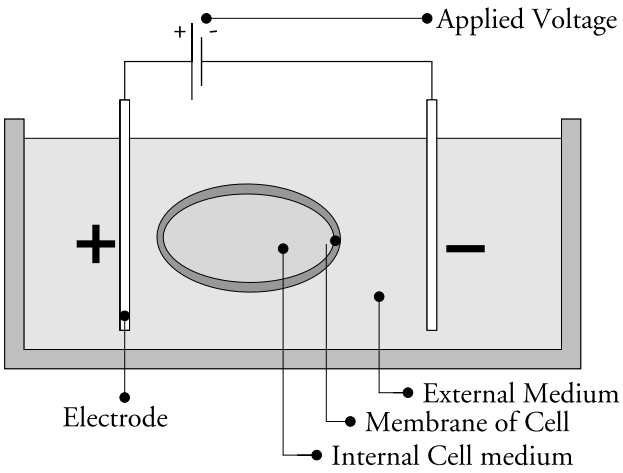

Figure 1: Typical electro-permeabilization experimental setup

theoretical model. For the purpose of this analysis it is assumed that the membrane of a cell is a simple medium of low conductivity, which has specific capacitance C_m of the order of $1\mu\text{F}\cdot\text{cm}^{-2}$. The membrane thickness is very small in comparison to the cell size and the dimensions of the external medium container. The size of the cell can vary greatly depending on the type of cell. A typical cell may have radius a of 1-100μm and a membrane thickness d several orders of magnitude smaller than the radius; typically 0.01μm.

In previous experimentations on balloon models [4, 6, 5] the external medium was a solution of domestic tap water with a conductivity of $14.3\times10^{-3}\text{S}\cdot\text{m}^{-1}$. However, in general, this value could be anywhere from distilled water $0.3\times10^{-3}\text{S}\cdot\text{m}^{-1}$ to an ionic solution with a much higher conductivity, depending on the concentration of the salts. The dielectric permittivity of distilled water is $81.1\epsilon_0 = 72\times10^{-9}\text{F}\cdot\text{m}^{-1}$. As biological cells have permeable membranes, the inside of the cell will have similar physical properties, at least within an order of magnitude.

The electric field $\mathbf{E}(\mathbf{x})$ prescribes how the current density $\mathbf{J}(\mathbf{x})$ flows through the conductive medium, with conductivity σ. The fields are assumed to obey Ohm's law

$$\mathbf{J} = \sigma\mathbf{E},$$

where $\mathbf{x}$ prescribes the location in space determined by a 3-tuple of Cartesian co-ordinates. The other vector field important to our investigations is the polarisation field $\mathbf{P}(\mathbf{x})$. This is related to the electric field through

$$\mathbf{P} = \chi\mathbf{E},$$

where the susceptibility $\chi = \epsilon_0(\epsilon - 1)$, and ϵ_0 and ϵ are respectively, the permittivity of free space, and the relative permittivity of the medium being considered.

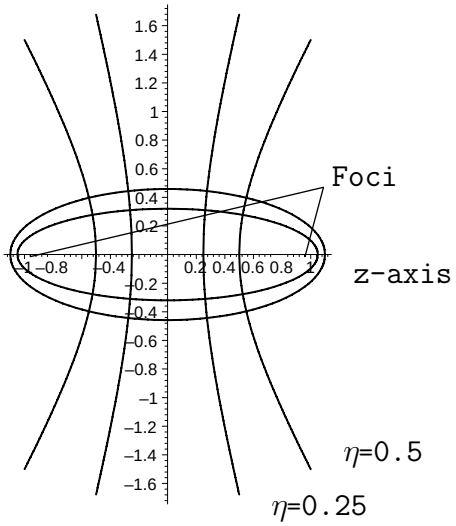

Figure 2: Co-ordinates of prolate spheroidal cell model with semi-focal distance $c = 0.8$, $d = 0.02$, and $\xi_o = 1.15$.

3 Prolate spheroid model

A prolate spheroid is essentially a distorted sphere. Consideration is given to the case of the electric field being parallel to the major axis as this is a comprehensive mathematical exercise in its own right. However in practice, experimental results [2, 7, 13] suggest that cells will align themselves either parallel or perpendicular to the field. Cells may also deform in either direction under an intense electric field depending on the ratio of the specific resistance of the external medium to that of the internal medium [1]. We shall consider only the parallel alignment case in this paper.

3.1 Coordinates

Elliptic coordinates are based on confocal ellipses, just as spherical coordinates are based on confocal circles, *e.*g. confocal ellipses are shown in Figure 2. Prolate spheroidal coordinates are formed by rotating elliptic coordinates around the major axis. The foci of the coordinates are set at $x = y = 0$, $z = \pm c$. A Cartesian point (x, y, z) can be uniquely expressed in terms of foci points $\pm c$, and the spheroidal coordinates $\{\xi, \eta, \phi\}$ as

$$\begin{aligned} z &= c\eta\xi, \\ x &= c\sqrt{(\xi^2 - 1)(1 - \eta^2)}\cos\phi, \\ y &= c\sqrt{(\xi^2 - 1)(1 - \eta^2)}\sin\phi, \end{aligned}$$

with latitude coordinate $\eta \in [-1, 1]$, and azimuthal angle $\phi \in [0, 2\pi]$.

The scalar factors for each of the co-ordinate differential lengths for the spheroidal

co-ordinates can be defined as ([11], pages 1284 *et.* seq.)

$$h_\xi = c\sqrt{\frac{\xi^2-\eta^2}{\xi^2-1}}, \quad h_\eta = c\sqrt{\frac{\xi^2-\eta^2}{1-\eta^2}}, \quad h_\phi = c\sqrt{(\xi^2-1)(1-\eta^2)}. \tag{3.1}$$

A prolate spheroid is the surface generated for ξ a constant. For the outer surface of the spheroidal cell, this will be denoted by ξ_o. The inner surface is described by ξ_i. The outer spheroid is set to have foci on the z axis at $\pm c$. The major axis is $c\xi_o$ along the z axis, and the minor axis $c\sqrt{\xi_o^2-1}$ on the x or y axes. If e is the eccentricity of the ellipse, with $e<1$, *i.e.* the ratio of the minor to the major axes of the ellipse, then $\xi_o = 1/\sqrt{1-e^2}$.

For the co-ordinate system based on confocal ellipsoids, there is a difficulty concerning the membrane thickness, as the distance between confocal ellipsoids is not constant. If d is used to denote the membrane thickness at the z-axis end of the spheroid, and when $d << 1$, it can be shown that the thickness in the middle of the spheroid is $d/e+\mathcal{O}((d/e)^2)$. This indicates that for a prolate spheroid, the membrane will be thicker at its middle when compared to the end caps; see Figure 2 or 3. However, such a varying membrane thickness may be representative of real cells under electric fields due to compressive forces. While the overall cell structure elongates, the membrane may thin at the major axis end regions. Mechanical compression in these regions has been offered as a mechanism by which electro-permeabilization might occur [2, 3]; although it was the subject matter of [4] to offer that dielectric breakdown rather than mechanical compression produced the holes in the membrane.

The inner surface of the membrane at ξ_i is used to select the membrane thickness at $\eta = \pm 1$, then $d = c(\xi_o - \xi_i)$, and ξ_o is chosen from $\xi_o = 1/\sqrt{1-e^2}$ where $c = a/\xi_o$ while a is the major axis of the ellipse.

3.2 Potential distribution

A spheroidal shell has a major axis a with $\xi_o = a/c$ and a membrane of thickness d at $\eta = \pm 1$ as shown in Figure 2 or 3. There are two boundaries between media, one at ξ_o, and the other at ξ_i.

For stationary fields the electric field can be represented by an electric potential, as $-\nabla\Phi$. For conducting media the divergence of the electric field is zero, so that the potential in the three regions of the medium is given by the solution to Laplace's equation. In prolate spheroidal co-ordinates ([11], Chapter 10) these solutions are of the form

$$\begin{aligned}
\Phi_i &= \sum_{l=0}^{\infty} a_l P_l(\xi) P_l(\eta), \quad 1 \le \xi < \xi_i, \\
\Phi_m &= \sum_{l=0}^{\infty} \Big(b_l P_l(\xi) + c_l Q_l(\xi) \Big) P_l(\eta), \quad \xi_i < \xi < \xi_o, \\
\Phi_o &= -E_0 c \xi \eta + \sum_{l=0}^{\infty} d_l Q_l(\xi) P_l(\eta), \quad \xi_o < \xi < \infty,
\end{aligned} \tag{3.2}$$

Quantity	Name	Units	Quantity	Name	Units
σ_i	intracellular conductivity	S/m	ρ_i	intracellular resistivity	Ω·m
σ_m	membrane conductivity	S/m	ρ_m	membrane resistivity	Ω·m
σ_o	extracellular conductivity	S/m	ρ_o	extracellular resistivity	Ω·m
R_m	membrane specific resistance	Ω·m^2	R_S	sphere model specific resistance	Ω·m^2
G_m	membrane specific conductance	S·m^{-2}	R_T	total leakage specific resistance	Ω·m^2
C_m	specific capacitance of membrane	F/m^2	ϵ_m	membrane relative permittivity	
ϵ_0	permittivity of free space	F/m	ϵ	relative permittivity	
χ	medium susceptibility	C/m^2			
a	major axis of spheroidal cell model	m	d	membrane thickness on major axis	m
e	eccentricity of prolate spheroid		c	semi-foci distance for ellipse	m
ξ_o	outer size of spheroidal cell		ξ_i	inner size of spheroidal cell	

List of Symbols

where: Φ_i, Φ_m, and Φ_o are the medium potentials, and ξ and η are the prolate spheroidal co-ordinates of any point in the medium, with respect to the foci at $\pm c$. The sequences $\{a_i\}$, $\{b_i\}$, $\{c_i\}$, and $\{d_i\}$ are constants associated with the particular fields. The form of the potential field generated by the uniform electric field is $\Phi = -E_0 z = -E_0 c\xi\eta$, and this has been used in the right-hand-side of (3.2). The functions $P_l(\xi)$ and $Q_l(\xi)$ are respectively, Legendre polynomials of order l, and Legendre functions of the second kind of order l; the latter possessing a singularity at $\xi = 1$.

By considering boundary conditions at $\xi = \xi_o$ and $\xi = \xi_i$, for respectively, the tangential electric field and the normal current density, the following equations are found

$$\left[\frac{1}{h_\eta}\frac{\partial\Phi}{\partial\eta}\right]_{\xi=\xi_o} = 0, \qquad \left[\frac{1}{h_\eta}\frac{\partial\Phi}{\partial\eta}\right]_{\xi=\xi_i} = 0,$$
$$\left[-\frac{\sigma}{h_\xi}\frac{\partial\Phi}{\partial\xi}\right]_{\xi=\xi_o} = 0, \qquad \left[-\frac{\sigma}{h_\xi}\frac{\partial\Phi}{\partial\xi}\right]_{\xi=\xi_i} = 0,$$

where the square brackets are used to denote jump conditions in the field quantities across the appropriate surface ξ =constant. Coefficients a_l, b_l, c_l, and d_l (for $l \neq 1$) are all zero by orthogonality of Legendre polynomials, and the coefficients a_1, b_1, c_1, and d_1 can be calculated, as shown in Appendix A.1. These remaining coefficients are listed in Appendix A.1 and are utilised in deriving the expressions used later in this subsection.

Hence the potentials are

$$\Phi_i = a_1\xi\eta, \quad 1 \leq \xi < \xi_i, \tag{3.3}$$
$$\Phi_m = \Big(b_1\xi + c_1 Q_1(\xi)\Big)\eta, \quad \xi_i < \xi < \xi_o, \tag{3.4}$$
$$\Phi_o = \Big(-E_0\xi c + d_1 Q_1(\xi)\Big)\eta, \quad \xi_o < \xi < \infty. \tag{3.5}$$

Equi-potential lines for a spheroidal model cell are shown in Figure 3(a) and the current flow is depicted in Figure 3(b). The equi-potential lines are uniformly spaced in potential.

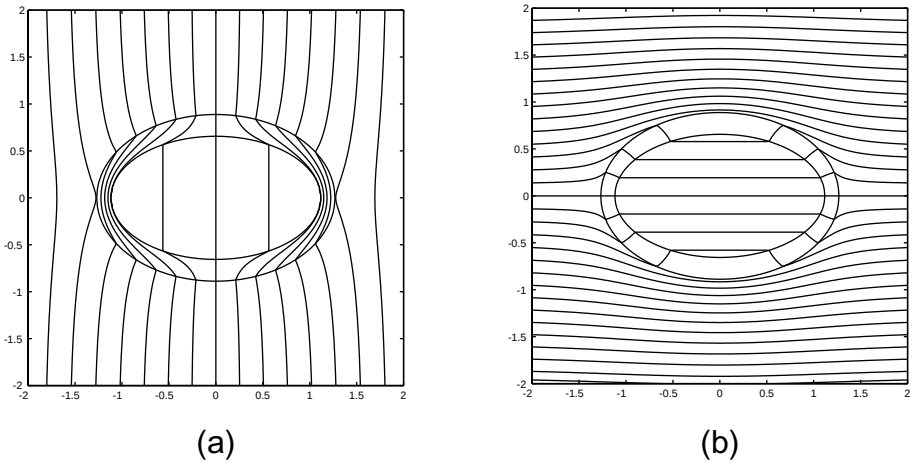

Figure 3: Fields for an exaggerated cell wall thickness model spheroidal cell; $d = 0.15$, $e = 0.70$: (a) Equipotential lines for a prolate spheroidal cell in a uniform electric field. (b) Current flow for a prolate spheroidal cell in a uniform electric field.

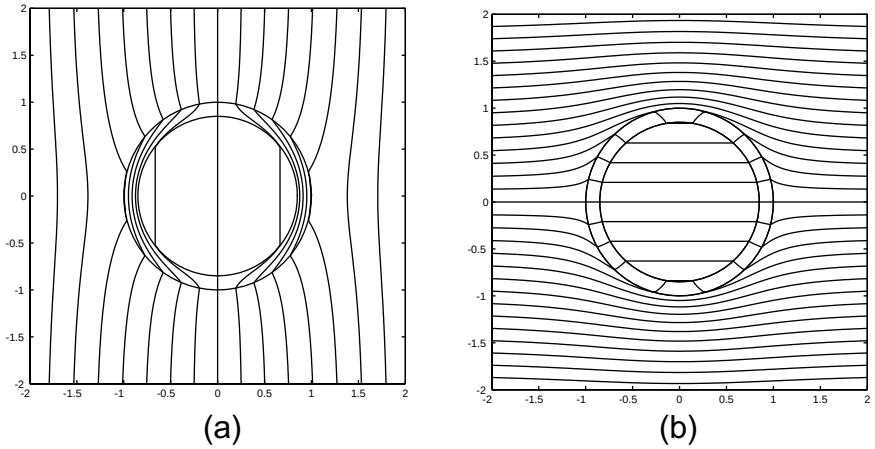

Figure 4: Fields for an exaggerated cell wall thickness model spherical cell; $d = 0.15$, $a = 1.0$: (a) Equipotential plot of a spherical cell in a uniform electric field. (b) Current flow for a spherical cell in a uniform electric field.

The cell used in this figure has a membrane conductivity of 1/20 of the external medium and the internal medium, *i.e.* $\sigma_m = \sigma_o/20$ and $\sigma_i = \sigma_o$; with $d/a = 0.15$. This figure should be compared with similar results for the spherical model as shown in Figure 4. The eccentricity of the spheroid is $e = 0.70$ and c has been adjusted so that the volume of the spheroidal cell is equal to that of the spherical cell. The spherical cell depicted has the same medium parameters and membrane thickness d as used in the spheroidal case. The spherical cell is assumed to have radius $a = 1.0$. Equi-potential lines for the spherical cell are shown in Figure 4(a) and the current flow for the cell is shown in Figure 4(b). In Figures 4(b) and 3(b), the lines of current flow are orthogonal to the equi-potentials.

A trans-membrane potential can be defined as the difference between the potential on the outside and inside of the membrane, so

$$\begin{aligned}\Delta_0\Phi(E_0) =&\Phi(\xi_o,\eta)-\Phi(\xi_i,\eta),\\ =&(-E_0c\xi_o+d_1Q_1(\xi_o)-a_1\xi_i)\eta,\\ =&-S_oE_0c\xi_o\eta f(\boldsymbol{\sigma}).\end{aligned}\tag{3.6}$$

Here the conductivity factor is

$$f(\boldsymbol{\sigma})=\left(1-\frac{d_1Q_1(\xi_o)}{E_0c\xi_o}+a_1\frac{\xi_i}{E_0c\xi_o}\right)/S_o,\tag{3.7}$$

and where for notational convenience we have defined the geometric factor

$$S_o=(1+Q_{oo}),\qquad\text{with}\quad Q_{oo}=\frac{-Q_1(\xi_o)}{\xi_oQ_1'(\xi_o)},$$

which is purely a function of the eccentricity of the spheroid and is shown in Figure 5. When $e=1$, $S_o=3/2$ and $Q_{oo}=1/2$, equation (3.6) reduces to equation (A.2) for the sphere. It is also observed that $\Delta_0\Phi$ is dependent on η, which is comparable to the $\cos\theta$ term described in the spherical membrane model in Appendix A.2.

The conductivity factor $f(\boldsymbol{\sigma})$ defined in (3.7), with $\boldsymbol{\sigma}$ denoting the triple $\sigma_o,\sigma_m,\sigma_i$, has the coefficients a_1 and d_1 defined in Appendix A.1. In Appendix A.1 it is shown that $f(\boldsymbol{\sigma})$ has an analytic form

$$f(\boldsymbol{\sigma})=\frac{\sigma_o\left(\frac{1}{Q_{io}}(\sigma_i-\sigma_m)-(\frac{\sigma_m}{Q_{ii}}+\sigma_i)+\frac{\xi_i}{\xi_o}\sigma_m(1+\frac{1}{Q_{ii}})\right)}{Q_{oo}\left[\frac{1}{Q_{io}}(\sigma_i-\sigma_m)(\sigma_m-\sigma_o)+(\frac{\sigma_m}{Q_{ii}}+\sigma_i)(\frac{\sigma_o}{Q_{oo}}+\sigma_m)\right]},$$

and terms Q_{ii} and Q_{io} are defined. When the membrane thickness d is small, an asymptotic expression can be found for $f(\boldsymbol{\sigma})$. Further, in the limiting case, $\sigma_m << \sigma_i$ and $\sigma_m << \sigma_o$ and d is small, this expression becomes

$$f(\boldsymbol{\sigma})=\frac{\sigma_m\sigma_od}{\left[\frac{1}{Q_{io}}(\sigma_i-\sigma_m)(\sigma_m-\sigma_o)+(\frac{\sigma_m}{Q_{ii}}+\sigma_i)(\frac{\sigma_o}{Q_{oo}}+\sigma_m)\right]}.$$

The above formulae should be compared with the similar and well known formulae for the sphere listed in Appendix A.2.

In Figure 6(a) the conductivity/resistivity factor is plotted for several spheroid eccentricities against $\log_{10}(\rho_m/\rho_i)$, when $\rho_o=\rho_i$ with a major axis thickness $d=0.01a$. It is seen that the eccentricity has only a small effect on the resistivity factor, and that the factor is more sensitive to membrane thickness when the spheroid is close to spherical. This can be seen from the curves plotted in Figure 6(b). In Figure 6(b) the resistivity factor is plotted

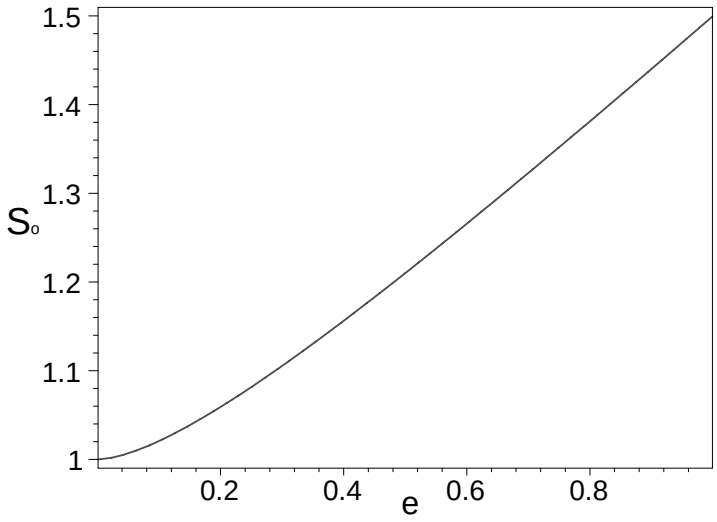

Figure 5: The geometric shape factor S_o as a function of spheroid eccentricity e.

for several membrane thicknesses for a comparison. It is observed, for the spheroid, for $d = 0.01$, and ρ_m three orders of magnitude greater than ρ_i, that f is approximately unity. For thicker membranes ρ_m need only be two orders of magnitude greater than ρ_i for $f \approx 1$.

We emphasize that the thickness of the cell membrane d is held fixed while consideration of eccentricity is made.

When $\sigma_m = 0$ it follows that $f(\boldsymbol{\sigma}) = 1$, and it is then seen from (3.6) that the potential difference produced across the membrane is

$$\Delta_0\Phi = -S_o E_0 c\xi_o \eta, \tag{3.8}$$

with maximum absolute value $E_0 c\xi_o S_o$. Because $c\xi_o = a$ is fixed, S_o varies as can be seen from Figure 5, it hence follows that $\Delta_0\Phi$ is dependent on the eccentricity e of the cell[2]. The η term in (3.6) implies that the maximal trans-membrane voltage is reached at the point of the cell closest to the electrode on the z axis, *i.e.*, $\eta = 1$, or -1, which is parallel to the applied electric field. The voltage across the membrane drops to zero, perpendicular to the applied field, and therefore electro-permeabilization will tend to occur in the vicinity of the cell membrane nearest the electrodes.

As $\xi_o = a/c$, it is seen that taking the limit as $c \to 0$ yields $S_o \to \frac{3}{2}$ (see also Figure 5) and equation (3.8) degenerates to the spherical model potential drop of equation (A.2). One immediate deduction therefore is that the trans-membrane potential is reduced with *narrower* spheroids and the *highest* potential difference is achieved with a *spherical* cell. This is because for the narrower spheroids the term S_o is less than 1.5 and can be as low as 1.

In Figures 7 and 8 we provide diagramatic evidence of this effect. Figure 7 shows a cell of constant volume, where the volume of the sphere and prolate spheroid are equal and are

[2]Through the dependence of the prolate spheroidal co-ordinates on e.

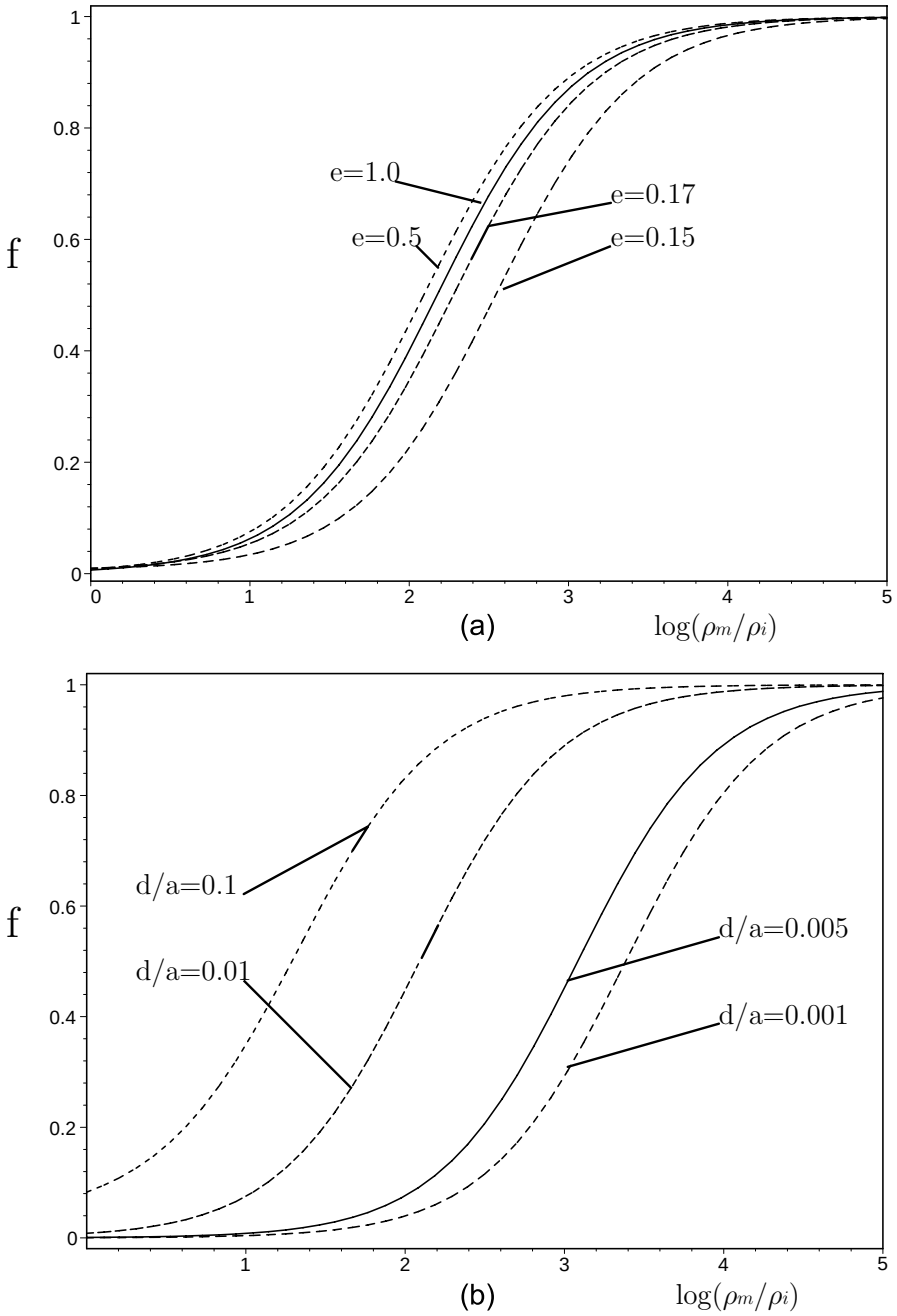

Figure 6: Conductivity factors $f(\boldsymbol{\sigma})$ as a function of spheroid eccentricity and membrane thickness for the prolate spheroid cell model when $\rho_o = \rho_i$. (a) $f(\boldsymbol{\sigma})$ for spheroid when $\sigma_o = \sigma_i$ and membrane thickness is $d/a = 0.01$ for $e = 1.0$, and $e = 0.5$, and $e = 0.17$, and finally with $e = 0.15$. (b) $f(\boldsymbol{\sigma})$ for spheroid when $\sigma_o = \sigma_i$ and membrane thickness $d/a = 0.001$, $d/a = 0.005$, $d/a = 0.01$, and $d/a = 0.1$, all with $e = 0.5$.

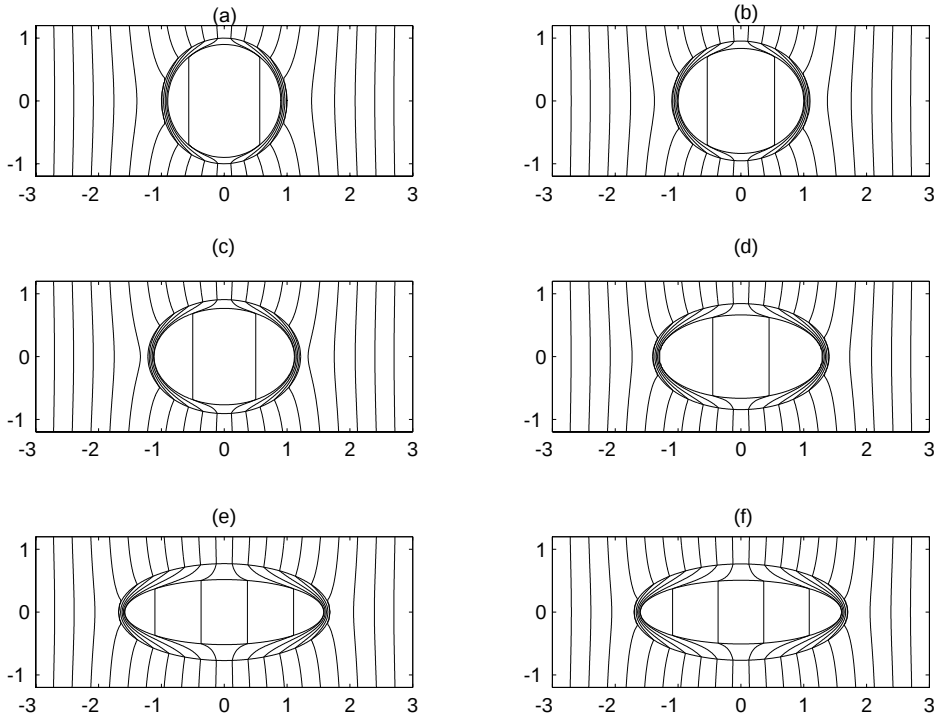

Figure 7: Equipotential fields for an equi-volume spheroidal cell when $\sigma_m = \sigma_o/20$ and $\sigma_i = \sigma_o$; with $d = 0.15$: (a) $c = 0$, $a = 1.0$ (b) $\xi_o = 2$, (c) $\xi_o = 1.5$, (d) $\xi_o = 1.25$, (e) $\xi_o = 1.125$, (f) $\xi_o = 1.12$.

given by

$$\begin{aligned} V &= \frac{4}{3}\pi a^3, \\ &= \frac{4}{3}\pi c^3 \xi_o(\xi_o^2 - 1), \end{aligned}$$

respectively. It is observed that as the eccentricity e is increased that the spheroid becomes longer (*i.e.* a is *not* constant). As a consequence this spheroid feels the effect of a *larger* electric field gradient. The potential can be crudely estimated by counting the number of equipotential lines emanating from the spheroid — as the lines are uniformly spaced with respect to potential. The trans-membrane potential can therefore be determined by differencing the equipotential lines outside and inside the cell.

For the major axis a being kept constant, as shown in Figure 8, it can be observed that the electric field gradient in the membrane is reduced on the narrower spheroids.

The electric potential generated at the poles of a spheroidal non-conducting cavity of size ξ_o embedded in a medium of conductivity σ_o under the same field E_0 is identical to the value given by (3.8). Note that the maximum trans-membrane potential depends linearly on f, and hence with a lower resistivity ratio ρ_m/ρ_i membranes (*c.f.* Figure 6), a higher potential E_0 is required to cause breakdown.

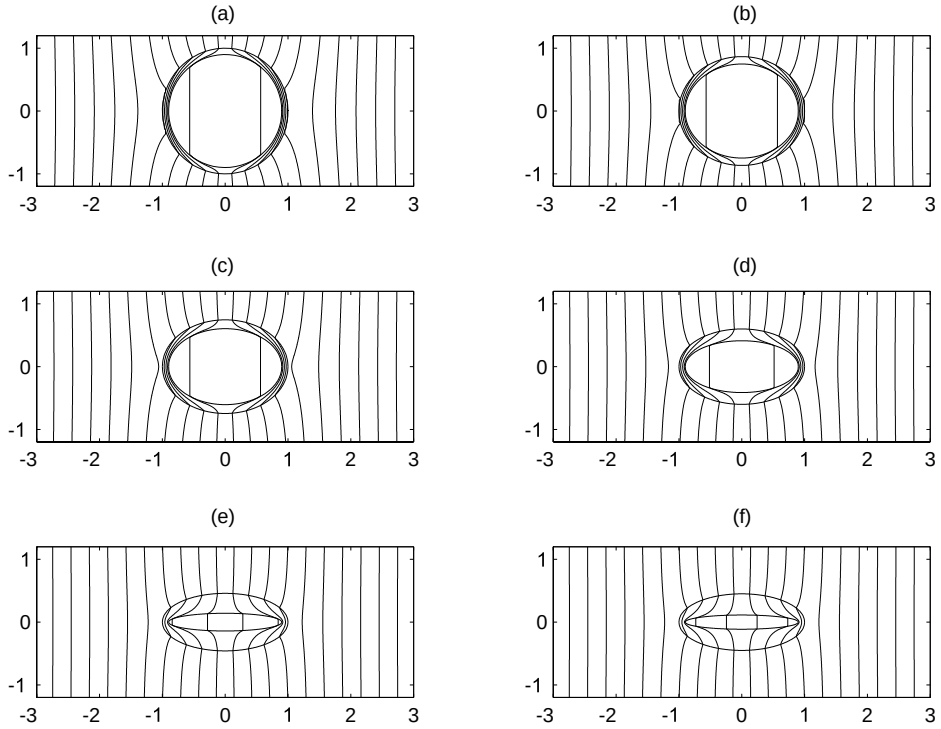

Figure 8: Equi-potential fields for a constant major axis spheroidal cell when $a = 1.0$, $\sigma_m = \sigma_o/20$ and $\sigma_i = \sigma_o$; with $d = 0.15$: (a) $c = 0$, (b) $\xi_o = 2$, (c) $\xi_o = 1.5$, (d) $\xi_o = 1.25$, (e) $\xi_o = 1.125$, (f) $\xi_o = 1.12$.

Many cells produce a natural trans-membrane voltage. This potential in the equilibrium state is caused by the thermodynamic forces (Nernst potential) enforcing an electrochemical balance due to the concentration gradient of chemical ions across the cell membrane. When the cell is not in equilibrium the trans-membrane potential can exhibit time varying features ([9], Chapter 4). Typically the natural transmembrane potential is the order of 70mV uniformly across the membrane with the interior of the cell being negative with respect to the exterior. As the potential differences add linearly it is seen that the potential difference across the membrane closest to the positive electrode will be larger than that nearest to the negative electrode, and that asymmetrical dielectric breakdown of the membrane will occur.

The analysis used in this section calculates the transmembrane potential due to the interfacial polarisation and is as such a stationary or static calculation. This can be a useful approximation when the temporal changes to the polarisation are slow and the displacement current can be neglected [12]. The time constant which can be used to calculate temporal behaviour is considered next.

3.3 Relaxation time constant

To take into account temporal changes in the polarisation charges that build up on the membrane of the cell it is required to estimate the macro specific resistivity enabling the leakage of this charge from the cell membrane. To this end we derive an approximate expression for this resistivity by setting $d \equiv 0$, or equivalently letting $\xi_i \to \xi_o$. Analysis of the spheroidal model in this case proceeds in a similar manner to the last section by excluding the potential Φ_m in the equations (3.2).

Solving Laplace's equation in this new geometry by similar techniques to those of § 3.1 yields

$$\begin{aligned}\Phi_i &= a_1 P_1(\xi)\eta,\\ \Phi_o &= \Big(- E_0 c\xi + d_1 Q_1(\xi)\Big)\eta,\end{aligned}$$

where now the field Φ_m is not present so that the set $\{b_i, c_i\}$ are trivially zero, and

$$\begin{aligned}a_1 &= - \frac{E_0 c\sigma_o S_o}{\Big(\sigma_o + \sigma_i Q_{oo}\Big)},\\ d_1 &= - \frac{E_0 c(\sigma_i + \sigma_o)}{Q_1'(\xi)\Big(\sigma_o + \sigma_i Q_{oo}\Big)}.\end{aligned} \tag{3.9}$$

The electric field normal to the spheroid is

$$E = \frac{1}{h_\xi}\frac{\partial \Phi_i}{\partial \xi} = -S_o E_0 c\xi_o \eta\left[\frac{\sigma_o}{\xi_o h_\xi(\sigma_o + \sigma_i Q_{oo})}\right],$$

and the current density normal to the spheroid is

$$\begin{aligned}J =& \sigma_i E,\\ =& - S_o E_0 c\xi_o \eta\left[\frac{\sqrt{\xi_o^2 - 1}\sigma_i\sigma_o}{\xi_o\sqrt{\xi_o^2 - \eta^2}(\sigma_o + \sigma_i Q_{oo})}\right].\end{aligned} \tag{3.10}$$

The jump in the normal component of the polarisation defines the polarisation surface charge density, denoted by ρ_S, and on the surface of the spheroid it is

$$\rho_S = - \chi E_0 S_o \eta\left[\frac{\sqrt{\xi_o^2 - 1}(\sigma_i - \sigma_o)}{\sqrt{\xi_o^2 - \eta^2}(\sigma_o + \sigma_i Q_{oo})}\right], \tag{3.11}$$

where the susceptibility $\chi = \epsilon_0(\epsilon - 1)$ is assumed to have the same value both inside and outside the spheroid. This charge density can be thought of as producing an internal field directly opposing the applied electric field so effecting the electric field inside the spheroid.

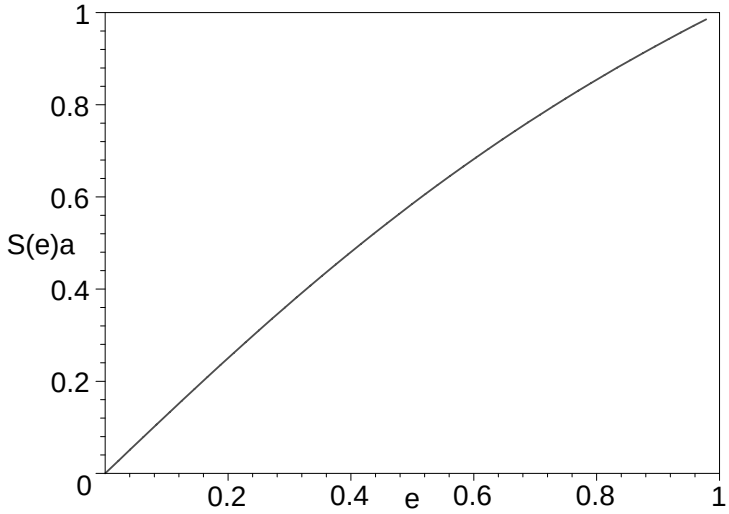

Figure 9: The geometric Shape factor $aS(e)$ as a function of spheroid eccentricity e.

Observe from these equations (3.9)–(3.11)that when the spheroid is needle shaped, *i.e.* $\xi_o \to 1$, that E, J and ρ will all be very large near $\eta = \pm 1$.

It can be seen by comparison of (3.10) with (3.8) that the term on the left-hand-side of (3.10), in square brackets, corresponds to an anisotropic leakage conductance varying with η. To eliminate the η variation, and so produce a circuit model of the charge leakage, it is necessary to average this density over the cap of the spheroid. This homogenisation of the current density will have an effect on the analysis of § 3.4 and this is discussed following equation (3.21). The homogenisation technique then yields a specific conductance, denoted by G_{PS}, to the leakage of surface charge from the end cap of a spheroid and it is given by

$$G_{PS} = 1/R_{PS} = S(\xi_o)\frac{\sigma_i \sigma_o}{(\sigma_o + \sigma_i Q_{oo})}, \tag{3.12}$$

with the eccentricity factor for the spheroid

$$S(\xi_o) = \frac{\sqrt{\xi_o^2 - 1}}{c\xi_o^2 F(\xi_o)}.$$

The generalised hypergeometric function F in this expression has an asymptotic expansion

$$F(\xi) = \left(1 - \frac{1}{6\xi^2} - \frac{1}{40\xi^4} + \mathcal{O}(\frac{1}{\xi^6})\right).$$

The size factor for the spheroid $S(\xi)a$ is plotted against eccentricity in Figure 9. Note in the limit as the spheroid reduces to a sphere, *i.e.* $e \to 1$, then $S(\xi_o) \to 1/a$ and $Q_{oo} \to 1/2$.

The equation (3.12) can be interpreted as determining the current leakage from two specific resistances $\rho_i/S(\xi_o)$ and $\rho_o Q_{oo}/S(\xi_o)$ connected in series, where $\rho_i = 1/\sigma_i$ and

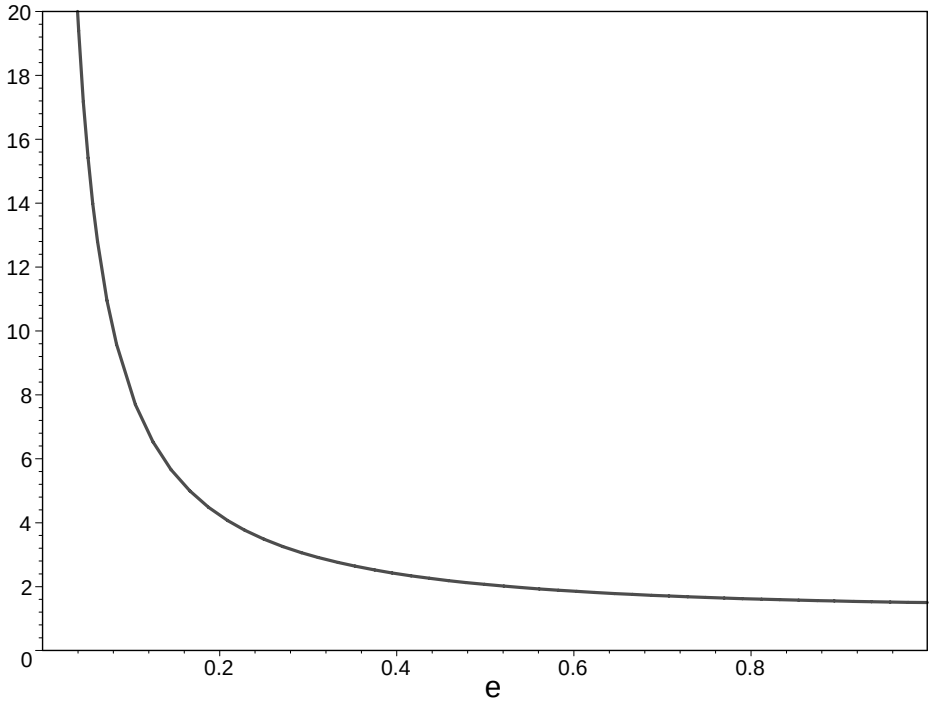

Figure 10: The normalised time constant $\tau_{PS}/C_m\rho_i$.

$\rho_o = 1/\sigma_o$. If the specific resistance of the membrane is denoted by $R_m = 1/G_m$, and as this resistance is in parallel with the former two, the total specific leak resistance, when denoted by R_T, is given by

$$\begin{aligned} R_T =& \frac{R_m R_{PS}}{(R_m + R_{PS})}, \\ =& \frac{R_m(\rho_i + Q_{oo}\rho_o)}{S(\xi_o)R_m + (\rho_i + Q_{oo}\rho_o)}, \\ =& \frac{(\sigma_o - \sigma_i Q_{oo})}{S(\xi_o)\sigma_i\sigma_o + G_m(\sigma_o + \sigma_i Q_{oo})}. \end{aligned}$$

Compare these formulae with the spherical model in Appendix A.2.

The capacitance per unit area associated with a spheroidal membrane can be calculated from the formula $C_m = \epsilon_0\epsilon_m/d$, where ϵ_0 is the permittivity of free space and ϵ_m the relative permittivity of the membrane.[3] This is an approximation in this model as the cell membrane in the spheroidal model has differing thickness. This formula is however correct to order d/a and this is a useful approximation as $d/a << 1$.

The time constant, which is a measure of how fast the charge carriers can move in response to the temporal excitation electric field, is then $\tau_{PS} = C_m R_T$. R_m is typically about two orders of magnitude larger than the leakage resistance *e*.g. $R_m = 10\Omega\cdot\mathrm{m}^2$, which

[3]For a lipid bilayer this is typically about 3.

means a useful approximation to τ_{PS} is

$$\tau_{PS} = C_m(\rho_i + \rho_o Q_{oo})/S(\xi_o). \tag{3.13}$$

Observe that the time constant can become very large as $e \to 0$ because of the $1/S(\xi_o)$ term in this equation and is shown in Figure 10.

3.4 Time dependence

The previous subsections enable calculation of the static polarisation charge build-up on the cell due to current flow through the medium. In this section we allow for temporal changes in the applied electric field.

When considering the effect of time dependence of an applied field it is obvious that a steady state is not achieved instantaneously. Thus there is a temporal redistribution of polarisation surface charge distribution on the spheroid; where it is assumed that this redistribution is a first order process governed by a time constant τ [12]. It is possible to find the equations governing the temporal changes in the trans-membrane potential difference from the dipole moment of the underlying polarisation of the media. This approach has been taken by [7, 5]. We take the more direct approach used by [12] of modeling the trans-membrane time behaviour of the interfacial potential difference directly.

The response function $p(t)$ is a first order process governed by a time constant τ. It can be assumed that the build up of p depends on the difference between the current state and the forcing function, $\widetilde{p}(t)$

$$\frac{dp(t)}{dt} = \frac{1}{\tau}(\widetilde{p}(t) - p(t)). \tag{3.14}$$

Solution of this equation yields

$$p(t) = \frac{1}{\tau}\int_{-\infty}^{t} \widetilde{p}(s)\exp[-\frac{t-s}{\tau}]\,ds, \tag{3.15}$$

with an initial condition $p(0) = 0$.

If the applied electric field varies as a function of time *i.e.*, $E_0 = E_0(t)$, then the polarisation is also temporally varying, and we can model the time variation in the trans-membrane potential by a process similar to equation (3.14). This means that the interfacial potential is

$$\Delta\Phi(t) = \frac{1}{\tau}\int_{-\infty}^{t} \Delta_0\Phi(E(s))\exp[-\frac{t-s}{\tau}]\,ds,$$

with $\Delta_0\Phi$ given by equation (3.6), and the appropriate time constant is $\tau = \tau_{PS}$. It follows that the build-up of the trans-membrane potential is

$$\Delta\Phi(t) = \Delta_0\Phi(E_0)(1 - \exp[-t/\tau_{PS}]), \tag{3.16}$$

when the applied electric field is the uniform field used in the last section and it is applied at time $t = 0$.

With the application of a sinusoidal electric field $E(t) = E_0 \cos \omega t$ into (3.15)

$$\Delta\Phi(t) = \frac{\Delta_0\Phi(E_0)}{1 + (\omega\tau_{PS})^2}(\cos \omega t + \omega\tau_{PS} \sin \omega t), \tag{3.17}$$

is obtained. Equation (3.17) has an amplitude

$$U = \frac{\Delta_0\Phi(E_0)}{\sqrt{1 + (\omega\tau_{PS})^2}}, \tag{3.18}$$

and if $(\omega\tau_{PS})^2 >> 1$, then (3.18) can be approximated by

$$U = \frac{\Delta_0\Phi(E_0)}{\omega\tau_{PS}}. \tag{3.19}$$

This approximation will be valid with high frequency excitation or when the cells are needle shaped (see Figure 10 which plots time constant against eccentricity of the cell).

Using the expression for τ_{PS} given in (3.13) in this equation shows

$$U = \frac{E_0\eta c\xi_o S_o f(\boldsymbol{\sigma})S(\xi_o)}{\omega C_m(\rho_i + \rho_o Q_{oo}))}. \tag{3.20}$$

The resistivity factor will reduce the amplitude of the trans-membrane potential if ρ_m is not large with respect to ρ_i and ρ_o. The thickness of the membrane will have a large effect on this factor when e is close to 1, whereas the eccentricity of the spheroid has a minor the effect as is shown in Figure 6(a).

Equation (3.20) is dependent upon both the size, though $c\xi_o = a$, and eccentricity, through $S(\xi_o)$ and Q_{oo}, of the spheroidal cell. However, if the resistivity of the external medium is chosen to match that of the internal cell, then $\rho_o = \rho_i$, and (3.20) becomes

$$U = -\frac{E_0\eta f(\boldsymbol{\sigma})aS(\xi_o)}{\omega C_m\rho_i}. \tag{3.21}$$

Equation (3.21) is independent of major axis size of the spheroid, but it is dependent upon the eccentricity of the prolate spheroid through $aS(\xi_o)$. However, from Figure 9, this term is roughly constant for $1 > e > 0.8$. Therefore, if either the frequency or the relaxation time constant is large enough, the size and shape dependence of the trans-membrane potential is eliminated for a range of prolate spheroids. This means that dielectric breakdown is possible at a constant field amplitude for a large range of prolate spheroidal cell shapes and sizes.

Notice again in this time dependent case, the deduction from equation (3.21) is that the trans-membrane potential is reduced with *narrower* spheroids and the *highest* potential is achieved with a *spherical* cell.

In the limit as $\xi_o \to 1$, the spheroid is eccentric, $e \to 0$, and the spheroid is *needle shaped*, then the polarisation charge density is located near to the end points $\eta = \pm 1$, with the charge density on the rest of the cell near to zero. This means the spheroid has a very small radius of curvature in the neighbourhood of the poles and this implies breakdown will occur very close to the poles prior to elsewhere on the cell membrane[4]. Then the term $aS(\xi_o)$ is very small in equation (3.21) for such cells thus implying the averaged trans-membrane potential is small for such cells. It should be observed that the term $S(\xi_o)$ resulted from the homogenisation utilised in deriving (3.12) and comes from the time constant τ_{PS} which is also very large in this case. Examination of (3.18) shows that large time constants will reduce the maximum amplitude potential difference and is to be expected. It should also be noticed though that the breakdown, even in the case of needle shaped cells, is independent of the cell size a.

4 Discussion

The membrane of the prolate spheroid model does not have uniform thickness due to the use of confocal ellipses. However, this may be representative of real cell behaviour under electric field induced compression forces.

Dielectric breakdown is a peak voltage phenomena and membrane thickness may be overlooked if only the maximum trans-membrane potential is of interest. Current flow through the cell peaks at the poles of the spheroid. This, and the assumption that the peak trans-membrane voltage is not affected by the variation in membrane thickness elsewhere on the cell, leads to the consideration that the effective membrane thickness is that at the poles.

The prolate spheroidal model could yield better predictions of non-spherical cell behaviour in electric fields. It may also provide more information into cell rotation and alignment, by considering the energy to form the dipole, both parallel and perpendicular to the applied field.

The model developed is based on a static electric field. The time dependence of these equations is only an approximation, valid at low frequencies where the displacement current is not dominant. Electro-permeabilization is generally carried out with time dependent fields and the cell membrane dielectric breakdown is generally size dependent. It is a current area of research to minimize this size dependence [5], and it has been shown in this paper how this can be achieved with prolate spheroid type cells that are *not too* elongated.

It has been shown that asymmetrical breakdown with cells having a natural trans-membrane voltage will occur.

[4]This is due to the η term in (3.21).

5 Conclusions

A spherical model of electro-permeabilization of biological cells has been extended to a prolate spheroid model, which is more representative of many real cells under actual electric field conditions.

The model yields the equi-potentials and current flow through the mediums which make up the cell cytoplasm, the membrane and the solution in which the cells are suspended. The highest potential difference across the membrane occurs at the cell ends along the major axis of the prolate spheroid. This gives rise to a charge polarization from which electro-permeabilization is likely to occur.

It has also been shown that for a range of eccentricities of the spheroidal model that electric breakdown can be arranged to occur independent of cell size and exact eccentricity. This may be useful in experimental usage of electro-permeabilization techniques.

Perhaps a surprising result emerging from this analysis is that the dielectric breakdown will occur at lower applied electric fields with more spherical shaped cells than with needle shaped cells.

References

[1] D. C. Chang, B. M. Chassy, J. A. Sanders, and A. E. Sowers, editors. *Guide to electroporation and electrofusion*. Academic Press, New York, 1992.

[2] H. G. L. Coster and U. Zimmermann. Dielectric electrical breakdown, in membranes of *Valonia Uticularis*: the role of energy dissipation. *Biochimica et Biophysica Acta*, **382**, 410–418, 1975.

[3] H. G. L. Coster and U. Zimmermann. The mechanisms of dielectric breakdown, in the membranes of *Valonia Uticularis*. *J. Membrane Biology*, **22**, 73–90, 1975.

[4] P. T. Gaynor and P. S. Bodger. Ionisation of dielectric spheroid membranes: a balloon model of electroporation of biological cells. *IEE Proc.-Sci. Meas. Technol.*, **141**(3), 190–196, May 1994.

[5] P. T. Gaynor and P. S. Bodger. Balloon model of biological cell electermeabilisation in relation to the radius dependence of membrane dielectric breakdown. *IEE Proc.-Sci. Meas. Technol.*, **142**(4), 277–22, July 1995.

[6] P. T. Gaynor and P. S. Bodger. Electrofusion processes: Theoretical evaluation of high electric field effects on cellular transmembrane potentials. *IEE Proc.-Sci. Meas. Technol.*, **142**(2), 176–182, March 1995.

[7] C. Holzapfel, J. Vienken, and U. Zimmermann. Rotation of cells in an alternating electric field: Theory and experimental proof. *Journal of Membrane Biology*, **67**, 13–26, 1982.

[8] J. D. Jackson. *Classical Electrodynamics*. John Wiley & Sons, Inc., New York, second edition, 1975.

[9] J. Keener and J. Sneyd. *Mathematical Physiology*, volume 8 of *Interdisciplinary Applied Mathematics*. Springer-Verlag, New York, 1998.

[10] J. C. Maxwell. *A Treatise on Electricity and Electromagnetism*. Oxford University Press, London, 3 edition, 1904.

[11] P. Morse and H. Feshbach. *Methods of Theoretical Physics*, volume 2. McGraw-Hill Book Company, New York, 1953.

[12] E. Neumann, A. E. Sowers, and C. A. Jordan, editors. *Electroporation and Electrofusion in Cell Biology*. Plenum Press, 1989.

[13] U. Zimmermann. Electric field-mediated fusion and related electrical phenomena. *Biochimica et Biophyisica Acta*, **694**, 227–277, 1982.

[14] U. Zimmermann. Electrical breakdown, electropermeabilization and electrofusion. *Rev. Physiol. Biochem. Pharamacol.*, **105**(6), 175–256, 1986.

A Appendix

A.1 Prolate model equations

In the case of the prolate spheroid, consideration of the boundary conditions yield

$$\begin{bmatrix} 1 & -1 & -Q_1(\xi_i)/\xi_i & 0 \\ \sigma_i & -\sigma_m & -\sigma_m Q_1'(\xi_i) & 0 \\ 0 & 1 & Q_1(\xi_o)/\xi_o & -Q_1(\xi_o)/\xi_o \\ 0 & \sigma_m & \sigma_m Q_1'(\xi_o) & -\sigma_o Q_1'(\xi_o) \end{bmatrix} \begin{bmatrix} a_1 \\ b_1 \\ c_1 \\ d_1 \end{bmatrix} = \begin{bmatrix} 0 \\ 0 \\ -cE_0 \\ -c\sigma_o E_0 \end{bmatrix}.$$

This has solutions

$$\begin{aligned}
a_1 &= \frac{cE_0}{D}\sigma_o\sigma_m\frac{Q_1(\xi_i)}{\xi_i}\frac{Q_1(\xi_o)}{\xi_o}\left(1+\frac{1}{Q_{ii}}+\frac{1}{Q_{oo}}+\frac{1}{Q_{ii}Q_{oo}}\right), \\
b_1 &= \frac{cE_0}{D}\sigma_o\frac{Q_1(\xi_i)}{\xi_i}\frac{Q_1(\xi_o)}{\xi_o}\left(\sigma_i(1+\frac{1}{Q_{oo}})+\frac{\sigma_m}{Q_{ii}}(1+\frac{1}{Q_{oo}})\right), \\
c_1 &= \frac{cE_0}{D}\sigma_o\frac{Q_1(\xi_o)}{\xi_o}(\sigma_m-\sigma_i)(1+\frac{1}{Q_{ii}}), \\
d_1 &= \frac{cE_0}{D}\frac{Q_1(\xi_o)}{\xi_o}\left((\sigma_m-\sigma_i)(\sigma_o+\frac{\sigma_m}{Q_{oo}})+\frac{Q_{i0}}{Q_{oo}}(\sigma_o-\sigma_m)(\sigma_i+\frac{\sigma_m}{Q_{ii}})\right), \\
D &= -\frac{Q_1(\xi_o)}{\xi_o}\frac{Q_1(\xi_i)}{\xi_i}\left[\frac{1}{Q_{io}}(\sigma_i-\sigma_m)(\sigma_m-\sigma_o)+(\frac{\sigma_m}{Q_{ii}}+\sigma_i)(\frac{\sigma_o}{Q_{oo}}+\sigma_m)\right].
\end{aligned}$$

where

$$Q_{io} = \frac{-Q_1(\xi_i)}{\xi_i Q_1'(\xi_o)}, \quad Q_{oo} = \frac{-Q_1(\xi_o)}{\xi_o Q_1'(\xi_o)}, \quad Q_{ii} = \frac{-Q_1(\xi_i)}{\xi_i Q_1'(\xi_i)}.$$

Note

$$P_1(x) = x, \quad Q_1(x) = \frac{x}{2}\ln\left(\frac{x+1}{x-1}\right) - 1,$$

and

$$Q_1'(x) = Q_0(x) - \frac{x}{x^2-1}, \quad \text{with} \quad Q_0(x) = \frac{1}{2}\ln\left(\frac{x+1}{x-1}\right),$$

with the equations for the Legendre functions holding for $x > 1$.

The conductivity factor is

$$\begin{aligned} f(\boldsymbol{\sigma}) =& \left(1 - \frac{d_1 Q_1(\xi_o)}{E_0 c \xi_o} + a_1 \frac{\xi_i}{E_0 c \xi_o}\right)/S_o \\ =& \frac{\sigma_o}{D} Q_{ii} Q_{io} \left(Q_{oo}(\sigma_i - \sigma_m) - (\frac{\sigma_m}{Q_{ii}} + \sigma_i) + \frac{\xi_i}{\xi_o}\sigma_m(1 + \frac{1}{Q_{ii}})\right) \end{aligned}$$

A.2 Spherical model

A spherical shell has a radius a and a membrane of thickness d. There are two boundaries between media, one at a, and the other at $a - d$. The potential at any point in the media is given by the solution to Laplace's equation ([10], pages 435-441) [8], and is of the form

$$\begin{aligned} \Phi_i &= \sum_{l=0}^{\infty} a_l r^l P_l(\cos\theta), \quad 0 \le r < a - d, \\ \Phi_m &= \sum_{l=0}^{\infty} b_l r^l + c_l r^{-(l+1)} P_l(\cos\theta), \quad a - d < r < a, \\ \Phi_o &= -E_0 r\cos\theta + \sum_{l=0}^{\infty} d_l r^{-(l+1)} P_l(\cos\theta), \quad a < r < \infty, \end{aligned} \tag{A.1}$$

where: Φ_i, Φ_m, and Φ_o are the medium potentials, and r and θ are the polar co-ordinates of any point in the medium, with respect to the sphere centre. The sequences $\{a_i\}$, $\{b_i\}$, $\{c_i\}$, and $\{d_i\}$ are constants associated with the particular fields. The form of the potential field generated by the uniform electric field is $\Phi = -E_0 z = -E_0 r\cos(\theta)$, and this has been used in the right-hand-side of (A.1).

Applying boundary conditions at $r = a$, and $r = a - d$, gives a set of equations which can be reduced by the orthogonality of the Legendre polynomials; all a_l, b_l, c_l, and d_l terms

with $l \neq 1$ must be zero. The remaining coefficients are listed in Appendix A.3 and are utilised in deriving the expressions in this appendix.

A trans-membrane potential can be defined as the difference between the potential on the outside and inside of the membrane, so

$$\begin{aligned}\Delta_0\Phi &= \Phi(a,\theta) - \Phi(a-d,\theta),\\ &= (-E_0 a + \frac{d_1}{a^2} - a_1(a-d))\cos\theta,\\ &= -\frac{3}{2}aE_0\cos(\theta)f(\boldsymbol{\sigma}),\end{aligned} \tag{A.2}$$

where the conductivity factor $f(\boldsymbol{\sigma})$ is defined as

$$\begin{aligned}f(\boldsymbol{\sigma}) =& \left(1 - \frac{d_1}{E_0 a^3} + a_1\frac{(a-d)}{E_0 a}\right)\frac{2}{3},\\ =& \frac{2\sigma_o\left(2\sigma_m + \sigma_i + (\sigma_m - \sigma_i)\left(\frac{a-d}{a}\right)^3 - 3\sigma_m\frac{a-d}{a}\right)}{(2\sigma_m+\sigma_i)(2\sigma_o+\sigma_m) + 2\left(\frac{a-d}{a}\right)^3(\sigma_i-\sigma_m)(\sigma_m-\sigma_o)}.\end{aligned}$$

This can be simplified by the approximation $d \ll a$, so implying

$$(\frac{a-d}{a})^3 = 1 - (3d)/a) + \mathcal{O}((d/a)^3),$$

which results in

$$f(\boldsymbol{\sigma}) = \frac{\sigma_i\sigma_o\big(2d/a\big)\frac{2d}{a}}{(\sigma_i+2\sigma_o)\sigma_m + (\sigma_i-\sigma_m)(\sigma_o-\sigma_m)(2d/a)\frac{2d}{a}}.$$

In the limiting case when $\sigma_m << \sigma_i$, $\sigma_m << \sigma_o$ then this expression becomes

$$f(\boldsymbol{\sigma}) = 1/\left[1 + (2 + \frac{\sigma_i}{\sigma_o})\left(\frac{a\sigma_m}{2d\sigma_i}\right)\right].$$

It can be seen from this equation when $\sigma_m = 0$ that $f(\boldsymbol{\sigma}) = 1$, it then follows from (A.2) that the maximum potential difference produced across the membrane is $-\frac{3}{2}E_0 a$. [5] It hence follows that $\Delta_0\Phi$ is always dependent on the radius a of the cell.

Analysis of the spherical model when $d \equiv 0$ yields the specific conductance to the leakage of charge from the surface of a sphere, denoted by G_S as

$$G_S = 1/R_S = \frac{\sigma_i 2\sigma_o}{a(\sigma_i + 2\sigma_o)},$$

this equation can be interpreted as leakage from two specific resistances $a\rho_i$ and $0.5a\rho_o$ in series where $\rho_i = 1/\sigma_i$ and $\rho_o = 1/\sigma_o$. It follows that when the specific resistance of the

[5] This is the potential generated at the pole of a spherical non-conducting inclusion of radius a in a medium of conductivity σ_o under the same field E_0.

membrane is denoted by $R_m = 1/G_m$ and it is reasoned that this resistance is in parallel with the former two, the total leak resistance is denoted by R_T and is given by [12, 5]

$$\begin{aligned} R_T =& \frac{R_m R_S}{(R_m + R_S)}, \\ =& \frac{a(\sigma_i + 2\sigma_o)}{2\sigma_i\sigma_o + aG_m(\sigma_i + 2\sigma_o)}, \\ =& \frac{R_m a(\rho_i + 0.5\rho_o)}{R_m + a(\rho_i + 0.5\rho_o)}. \end{aligned}$$

A.3 Spherical model equations

The boundary conditions for the spherical membrane model, can be solved by rearranging the conditions and placing them in matrix format:

$$\begin{bmatrix} 1 & -1 & -(a-d)^{-3} & 0 \\ \sigma_i & -\sigma_m & 2\sigma_m(a-d)^{-3} & 0 \\ 0 & 1 & a^{-3} & -a^{-3} \\ 0 & \sigma_m & -2\sigma_m a^{-3} & 2\sigma_o a^{-3} \end{bmatrix} \begin{bmatrix} a_1 \\ b_1 \\ c_1 \\ d_1 \end{bmatrix} = \begin{bmatrix} 0 \\ 0 \\ -E_0 \\ -\sigma_o E_0 \end{bmatrix},$$

This matrix equation has solutions

$$\begin{aligned} a_1 &= \frac{-E_0}{D} 9\sigma_o\sigma_m a^3, \\ b_1 &= \frac{-E_0}{D} 3E_0 a^3 \sigma_o(2\sigma_m + \sigma_i), \\ c_1 &= -\frac{E_0}{D}(\sigma_m - \sigma_i)(a-d)^3, \\ d_1 &= \frac{E_0}{D} a^3(-3\sigma_m a^3\sigma_o - 3\sigma_i a^2 d\sigma_o + 3\sigma_m a^2 d\sigma_o - 6\sigma_m\sigma_i a^2 d + 3\sigma_m\sigma_i a^3 + 3\sigma_i a d^2\sigma_o \\ &\quad + \sigma_m d^3\sigma_o + 6\sigma_m\sigma_i a d^2 - 3\sigma_m a d^2\sigma_o - \sigma_i d^3\sigma_o + 6\sigma_m^2 a^2 d - 2\sigma_m\sigma_i d^3 \\ &\quad - 6\sigma_m^2 a d^2 + 2\sigma_m^2 d^3), \end{aligned}$$

where

$$D = \frac{1}{a^6(a-d)^3}\left[(2\sigma_m + \sigma_i)(2\sigma_o + \sigma_m) + 2\left(\frac{a-d}{a}\right)^3(\sigma_i - \sigma_m)(\sigma_m - \sigma_o)\right].$$